Unspecified Journal
Volume 00, Number 0, Pages 000–000
S ????-????(XX)0000-0

VISION BASED HAPTIC FEEDBACK FOR REMOTE MICROMANIPULATION IN A SEM ENVIRONMENT

AUDE BOLOPION[*,1], CHRISTIAN DAHMEN[*,2], CHRISTIAN STOLLE[*,2], SINAN HALIYO[3], STÉPHANE RÉGNIER[3] AND SERGEJ FATIKOW[2]

ABSTRACT. This paper presents an intuitive environment for remote micromanipulation composed of both haptic feedback and virtual reconstruction of the scene. To enable non expert users to perform complex teleoperated micromanipulation tasks it is of utmost importance to provide them with information about the 3D relative positions of the objects and the tools. Haptic feedback is an intuitive way to transmit such information. Since position sensors are not available at this scale, visual feedback is used to derive information about the scene. In this work, three different techniques are implemented, evaluated and compared to derive the object positions from scanning electron microscope images. The modified correlation matching with generated template algorithm is accurate and provides reliable detection of objects. To track the tool, a marker based approach is chosen since fast detection is required for stable haptic feedback. Information derived from these algorithms is used to propose an intuitive remote manipulation system, that enables users situated in geographically distant sites to benefit from specific equipments such as SEMs. Stability of the haptic feedback is ensured by the minimization of the delays, the computational efficiency of vision algorithms and the proper tuning of the haptic coupling. Virtual guides are proposed to avoid any involuntary collisions between the tool and the objects. This approach is validated by a teleoperation involving melamine microspheres with a diameter of less than 2 μm between Paris, France and Oldenburg, Germany.

[*]A. Bolopion, C. Dahmen and C. Stolle contributed equally to this work.
[1]A. Bolopion is with Institut FEMTO-ST, UFC, ENSMM, UTBM, CNRS UMR 6174, 24 rue Alain Savary, 25000 Besançon, France. aude.bolopion@femto-st.fr.
[2]Authors are with Division Microrobotics and Control Engineering, Oldenburg University, Oldenburg, Germany. christian.stolle@uni-oldenburg.de.
[3]Authors are with Institut des Systèmes Intelligents et de Robotique, Université Pierre et Marie Curie - Paris 6, CNRS UMR 7222, 4 Place Jussieu, 75005 Paris, France. {haliyo, regnier}@isir.upmc.fr.

1. INTRODUCTION

Versatile micromanipulation systems would open a wide range of applications, that would benefit different areas, such as medicine, electronics or physics. To enable non expert users to perform micromanipulation tasks intuitiveness of the system is a major requirement. In particular it is necessary to provide users with information about the 3D relative positions of the tools and the objects. So that intuitiveness is ensured it is possible to enhance the visual feedback by reconstructing virtual scenes [14, 10]. In addition to visual display haptic feedback can be provided. Operators manipulate the tools through a joystick, and receive force feedback [6, 25]. To provide such assistance sensing capabilities are necessary to get information about the scene. Specific sensors, adapted to microscale requirements, have been developped [9, 1]. However, their integration into the dedicated tools is complex, and greatly increases the difficulty of their design and their conception. Vision is thus a promising solution to compensate for this lack of sensing [13, 18, 19, 7].

Visual feedback obtained from classical optical microscopes is limited to objects whose size is greater than a few micrometers. To manipulate smaller objects specific equipments, Scanning Electron Microscopes (SEM), must be used to visualize the scene. For detection and tracking of objects and tools in SEM images, common algorithms include rigid-body based matching [15], active contours [20] and template matching using cross correlation [21]. Though these algorithms are flexible and robust, not all of them are suitable for the simultaneous detection of a high number of simple objects, like melamine spheres. They must also be computationally efficient to provide haptic feedback and real time reconstruction of the virtual scene.

In this work three different detection algorithms are implemented, evaluated and compared in terms of computation time, accuracy and reliability. To provide haptic feedback and real time reconstruction of the scene the modified correlation matching with generated template algorithm is used to get information about object positions. To track the tool, a marker based approach is chosen since fast detection is required. As the proposed detection algorithms are computationally efficient, they can be used to provide an intuitive remote teleoperation environment with stable haptic feedback. To validate this approach, a

teleoperated task involving microspheres is performed between France and Germany. The haptic feedback teleoperation system is detailed. A special care has been taken to ensure stability by minimizing the communication delays and the vision detection computation time. Virtual guides are proposed to avoid any involuntary collision between the objects and the tool, by the transmission of adapted haptic feedback. A paper describing the software architecture of this system, that ensures the minimization of time delays as well as modularity, has been published in [3]. The work presented here concentrates on computationally efficient and robust detection algorithms for SEM images in order to propose vision-based haptic feedback and virtual reconstruction of the scene. Another approach is presented in [4], where the relative position of the tool (a cantilever) and the objects is derived from direct measurement: the cantilever is excited at its resonant frequency, and the amplitude of the oscillations is monitored. It decreases while the cantilever approaches an object. However, it requires bringing the cantilever in the close vicinity of the object, and it does not give indication about the whole scene. In particular, it is not possible to provide an updated virtual reconstruction of the scene during the manipulation task based on direct measurements.

This paper is organized as follows. Section 2 describes the micromanipulation system. Vision algorithms, adapted to the specificities of SEM images, are proposed in Section 3 to track both the tool and the objects. Based on the position information derived from these algorithms, an intuitive manipulation system composed of both a virtual scene reconstruction and haptic feedback is proposed in Section 4. This approach is validated by experiments conducted on microspheres using teleoperation between France and Germany.

2. MICROMANIPULATION PLATFORM

2.1. **Setup.** Cantilevers are widely used inside Atomic Force Microscopes (AFM) to manipulate micron-sized objects since they are commercially available and rather cheap. Several strategies have been developed, such as pushing, rolling, or pick-and-place by adhesion, or by using two tips as a microgripper [25]. To derive interaction forces involved

while manipulating objects the deformations applied on the cantilever are measured , either by using optical systems composed of lasers reflected on photodiodes, or by using piezoresistive sensors. However, these measurements are mostly limited to the vertical deflection of the cantilever, which is related to a vertical force applied on the tool. Due to the design of the cantilever, the resolution of torsional forces is too low to be used as force feedback for a manipulation task. In this work a commercially available piezoresistive contact type cantilever[1] with a stiffness of 4 $N.m^{-1}$ is used. Vertical forces applied on the cantilever are translated into a change in resistance and measured as voltage change. Voltage measurements are made using an amplifier[2] and a 16-bit analog digital converter[3].

The cantilever is used to manipulate commercially available melanin microspheres[4] (diameter: $1 - 1.6$ μm) loosely deployed on a silicon plate (5 mm x 5 mm). It is mounted on the fine positioning part of a nanorobotic setup [16]. This positioning part is piezo driven with a build-in capacitive position sensors for closed-loop movement control and high accuracy positioning[5]. Its lateral stroke is up to 100 μm and the z-range is up to 50 μm and the positioning accuracy is at the lower nanometer scale. The specimen holder has been mounted on a coarse positioning unit. This unit consists of three slip stick driven, orthogonal mounted linear axes[6]. These positioners are equipped with optical positioning sensors allowing for travel ranges of several centimeters with a repositioning accuracy up to 50 nm.

The whole setup is placed inside a high-resolution scanning electron microscope with a Schottky-emitter[7] that is also equipped with a FIB column[8] and a gas injection system. Such microscopes provides images of objects smaller than a few micrometers, sufficiently precise to determine the relative position of the tool and the objects for manipulation tasks. This information is used in this work to set up an intuitive remote micromanipulation platform.

---

[1]SSI-SS-ML-PRC400, Seiko Instruments
[2]Hottinger Baldwin Messtechnik GmbH
[3]NI-PCI-6259, National Instruments
[4]Micro Particles GmbH
[5]Physikinstrumente GmbH
[6]SmarAct GmbH
[7]Lyra2, Tescan
[8]Canion, Orsay-Physics

The teleoperation platform is composed of an Omega haptic device[9] used to control the position of the cantilever. A haptic feedback is sent through the device to assist operators while manipulating objects. This master arm is a 3 degrees of freedom device for both displacement and haptic feedback. To avoid damages of the haptic interface forces higher than 3 N are truncated. Users are also immersed in a virtual reality room which comprises a 3D display module. A reconstructed image of the scene is projected in stereoscopic 3D on a 1.80×2.4 m^2 screen.

2.2. **Software Architecture.** The robotic control system is based on the distributed control system for automated micro- and nano robotics (DCAAN) [22]. It consists in several servers written in C++ which are connected via CORBA (Common Object Request Broker Architecture) based on a TCP/IP network. Due to the distributed nature of the tele-control task the software has been subdivided into two parts (see Fig. 1). The one located in Paris is the operator side, and the one in Oldenburg is the manipulation setup. At the remote side three different programs are running:

- the sensor provider Olvis is responsible for processing image based information such as video streams [24]. Depending on these algorithms different kinds of information such as sphere and cantilever positions can be derived (see Section 3),
- the AFM low level control server is processing the tele-control commands by moving the cantilever tip to the target position and sending an estimation of the actual position and a measure of the force back in return,
- the SEM low level control server enables in particular the operator to turn the experimental setup towards the focus of the SEM by moving the SEM stage, and to change image parameters such as brightness and contrast. These settings are indeed of primary importance to ensure efficient vision tracking and detection.

[9]Force Dimension, http://www.forcedimension.com

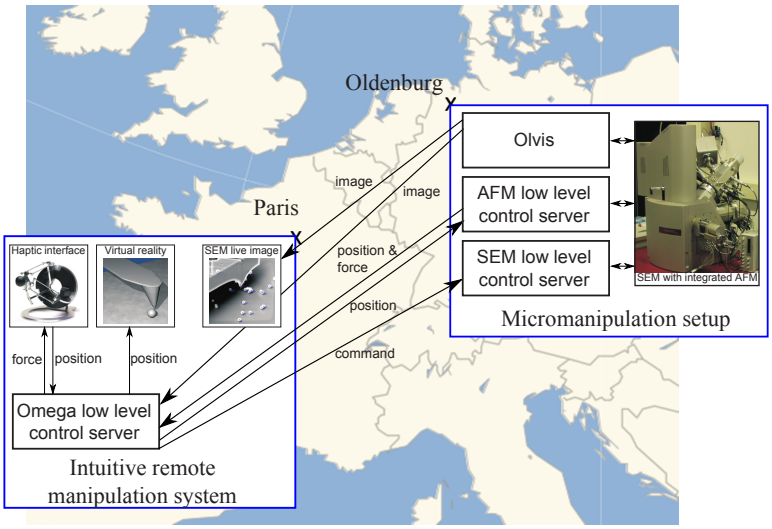

FIGURE 1. Software architecture and communication layout between the remote side in Oldenburg and the operator side in Paris

The Omega low level control server forms the heart of the operator side software and provides a small graphical user interface which enables the operator to monitor information such as force and position of the cantilever. In addition to the numerical display a live SEM image (see Section 3) can be provided to the operator via the GUI. The Omega low level control server is also responsible for translating the force and position feedback of the AFM-cantilever and forces and positions of the haptic device into each other.

The communication between the operator and the remote sides has been realized directly via UDP packages. The communication delay has been measured by the means of the round trip time (RTT) by requesting the current position of the cantilever 100 times. The average RTT has been determined at 37 ms, the minimum RTT at 36 ms and the maximum RTT at 39 ms. The distributed control system enables to minimize RTT, and to ensure modularity. It is thus suitable to perform a wide range of teleoperation over important distances.

3. SEM BASED VISION ALGORITHMS FOR TRACKING AND DETECTION

In SEM-based micro- and nanorobotic handling, visual feedback from the SEM is one of the main sources of information about the workspace. The SEM feedback is used during the registration process where the positions of parts and robot tools are determined, as well as for position feedback during the handling process itself. The SEM as sensor itself introduces some constraints on detection and tracking algorithms, which must be adapted to the specifics of SEM images. These constraints include e.g. robustness against stochastic additive noise and changes in brightness or contrast. In addition the update rate must be sufficient to meet the requirements of haptic feedback. In our setup the images are acquired with a resolution of 627 x 627 pixels. The field of view for the handling scene is in the range of 10 to 100 μm.

The cantilever is tracked with a template matching algorithm (TM) [12], which is one of the fastest and the most common real-time marker tracking approaches. It finds the position in the image with the best correspondence with the template. To achieve good tracking results, a marker has been structured by the FIB on top of the cantilever. This marker is used as the template for the TM, and its unique features enable to precisely determine the position of the cantilever. In the initialization step the marker is tagged manually. Automated detection will be considered in future works. To calculate the position of the cantilever tip, a offset is added to the position of the tracking marker. To be used in teleoperation, the update rate of the position of the cantilever has to be as fast as possible. Therefore the process is set to the highest priority in the Olvis framework to achieve an update rate of up to 50 Hz.

The detection of the melamine spheres is more difficult in contrast to the cantilever because the appearance of the spheres changes during the handling (Fig. 2). The cantilever shadows the spheres due to position changes, which modifies the intensity and contrast of the image. Due to the view angle depended detector shadowing effects and different brightness and texture features of the spheres, it has been decided to work on edge images to generate comparable results. Algorithms applied to this scenario need to be developed

to especially meet these requirements. For this purpose three different detection methods have been selected, tested and compared:

- Contour detection with circle fitting criteria's,
- Modified correlation matching with generated templates,
- Hough circle detection.

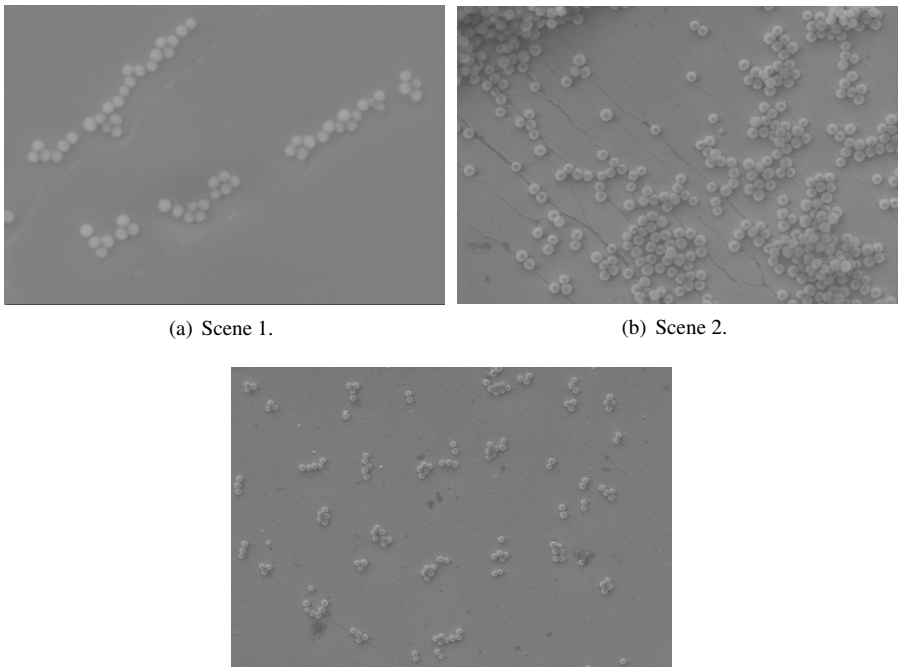

(a) Scene 1. (b) Scene 2.

(c) Scene 3.

FIGURE 2. Example images of melamine spheres imaged with the SEM. Three different scenes have been used for evaluation.

The first approach uses contour detection with circle fitting criteria. After the edge detection is applied, the contours are detected using the OpenCV [5] contour detection (cvContour) and ellipse fitting (cvFitEllipse2) functions. As a result, a number of found contours with different parameters are returned. To find the contours, which are mostly fitting a sphere, different criteria have to be calculated:

- Roundness deviation error (RDE) of the contour in comparison to the calculated radius

$$RDE = \sum_{ContourPoints} \left(1 - \left(\frac{x^2}{a^2}\right) + \left(\frac{y^2}{b^2}\right)\right) \tag{3.1}$$

where

$$a = \frac{BoundingBox.width}{2}$$

$$b = \frac{BoundingBox.height}{2}$$

$$x = ContourPoint.x - BoundingBox.center.x$$

$$y = ContourPoint.y - BoundingBox.center.y,$$

- Width-to-height-ratio ($Ratio_{WH}$) of the bounding box

$$Ratio_{WH} = \frac{BoundingBox.width}{BoundingBox.height}, \tag{3.2}$$

- Area (A) of the bounding box, to limit the diameter search range of the spheres,
- Number of segments.

These four criteria are used to calculate a score. After applying a threshold to filter the scores, a list of validly detected sphere contours is given and the center points are calculated.

The second approach uses modified cross correlation (CC) [12] with generated templates, similar to the ones applied during cantilever tracking. After applying the edge detection filter a CC is used to find the spheres. The formula beneath shows the mathematical basics of the used normalized cross correlation function (NCCF). In the formula $w(u,v)$ are pixel values in the correlation window and $G(x,y)$ are the pixel values from the search region with l and k smaller then the image size m x n of the CC function (CCF):

$$CCF(x,y) = \sum_{u=0}^{l-1} \sum_{v=0}^{k-1} w(u,v) * G(x+u, y+v). \tag{3.3}$$

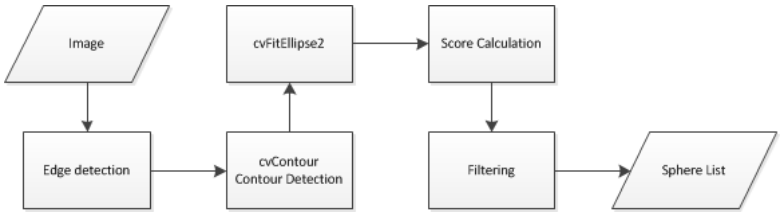

(a) Contour detection based algorithm.

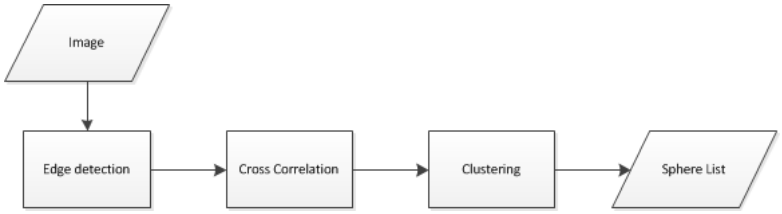

(b) Cross correlation based algorithm.

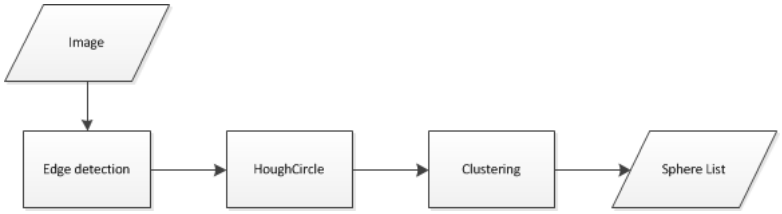

(c) HoughCircle based approach.

FIGURE 3. The three used algorithms, contour detection based, cross correlation based, and HoughCircle based.

The normalization term (NT) is

$$NT(x,y) = \sqrt{\sum_{u=0}^{L-1}\sum_{v=0}^{K-1} w(u,v)^2} * \sqrt{\sum_{u=0}^{L-1}\sum_{v=0}^{K-1} G(x+u,y+v)^2}. \tag{3.4}$$

Finally,

$$NCCF(x,y) = \frac{CCF(x,y)}{NT(x,y)}. \tag{3.5}$$

In contrast to normal CC templates, binary ring templates are used. These ring templates are specially generated to fit to the contour of a circle, independently of the texture values of the sphere. Therefore, a list of ring templates with different radii and ring widths are automatically generated and passed to the CC. Finally, the result list is clustered and the weighted center points are calculated. The clustering is necessary, because the same sphere can be multiply detected on a slightly different position in each CC cycle.

The third approach uses a Hough circle detection [11] on an edge image with different radii. Therefore a modified version was implemented. For the same reason as described in the CC approach, the result list has to be clustered and finally the weighted center points of the detected spheres are calculated. The Clustering of all three methods was done by using the OpenCV function (cvSeqPartition).

All three methods have been evaluated with respect to the special requirements of AFM-based sphere handling inside the SEM. The contour detection method offers fast computation time which is necessary for teleoperation (otherwise haptic feedback is unstable [8]). The disadvantages of this method are high false detection rates, due to increasing image noise and comparatively small spheres.

The CC with ring templates and the Hough circle detection both have a higher computation time in comparison to the contour detection method. Their advantage is higher accuracy and better reliability. On the one hand, the CC with ring templates has a higher reliability in blurry images and images with many small spheres but on the other hand, the Hough circle detection has the better computation time. Currently the computation time is in the range of 0.4 s to 2 s, depending on the density of input edge images. Another advantage of these two methods is that their algorithms can be scheduled in parallel. Currently both algorithms are implemented in OpenCl [23] to work on graphic card units and to optimize the calculation time.

In Figure 4, results of sphere detection of the scenes of Fig. 2 using hough circle detection can be seen. Marked are true positives in green, false positives in blue, and false negatives in red. The successful and failed detection have been determined by hand. The results of the evaluation can be seen in Table 1. As can be seen, the false positives are relatively low count. This can be still improved by further optimization of the parameters. The main errors are false negatives, which clearly depend on the various factors influencing the image as stated before.

To meet the teleoperation requirements of fast and accurate detection, as well as reliability, the CC based approach has been used for the handling experiments. In particular, the

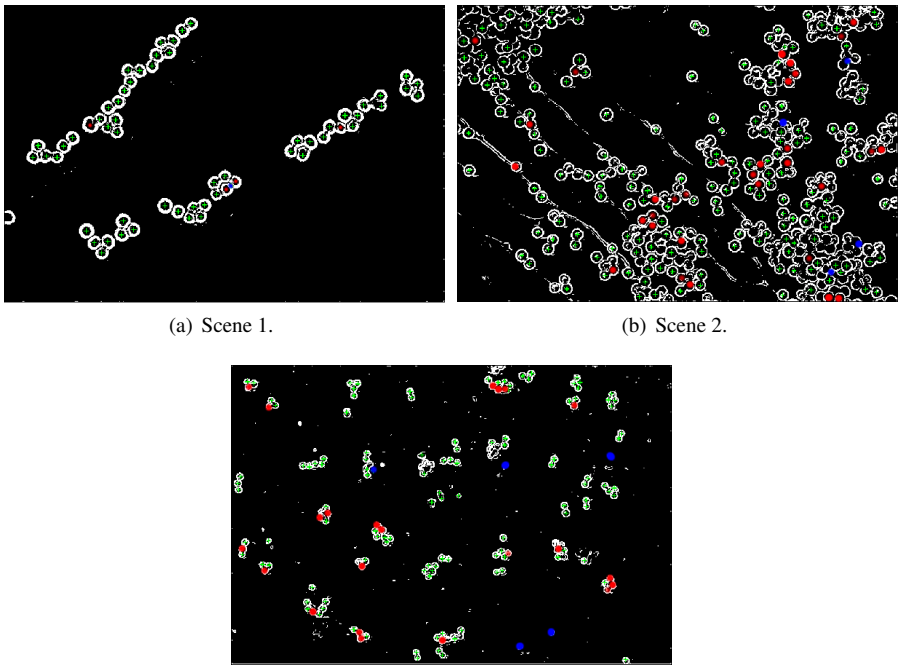

(a) Scene 1. (b) Scene 2.

(c) Scene 3.

FIGURE 4. Example images of the edge detected images with true positives, false positives and false negatives determined by the algorithm marked with color. Green: true positives, blue: false positives, red: false negatives.

Scene	No. of Spheres	True Positives	False Positives	False Negatives
1	59	55 (93,2%)	1	4
2	216	168 (77,7%)	6	48
3	136	115 (84,6%)	5	21

TABLE 1. Results of the evaluation from the three scenes using hough circle approach (see Figure 4).

algorithm integrates SEM parameters like view field to achieve a magnification invariant detection. However, in order to avoid a slowdown of the cantilever tracking, the positions of the melamine spheres are calculated with a low priority in the Olvis framework. This choice was made since the cantilever is moved more often than the spheres. The sphere detection has an update rate of 3 to 8 Hz for searching in the sphere diameters in the range of 1 to 1.6 µm. This detection algorithm, as well as the one for the cantilever detection,

have a sub-pixel accuracy.

During this application the position of the involved objects was only determined in x and y directions of the SEM image plane. The relative height of the cantilever with respect to the substrate is thus unknown. For this work, this lack of information is compensated by the force measurement of the piezoresistive sensor, which estimates the vertical force applied on the cantilever and enables to determine if the tip is or not in contact with the substrate or an object. However, this method does not compensate for the unknown orientation of the substrate surface and the image plane. This may lead in turn to an ellipsoidic shaped force gradient while the cantilever is in contact with the surface. One solution would be to include a calibration step, or image processing based on the distance between the tip and its shadow on the substrate.

4. Intuitive Teleoperation Environment

Based on the position information of the tool with respect to the object that is derived by vision algorithms, an intuitive remote manipulation system is proposed. It is composed of both visual and haptic feedback. Intuitive remote manipulation systems will enable non expert users to get access to rare and expensive equipments, that are often situated in geographically distant sites.

4.1. The Intuitive Remote Manipulation System.

To assist users while performing a manipulation, a stereoscopic virtual reality scene is reconstructed using *Blender*, an open source 3D content creation suite [2]. The scene includes the AFM tip used as the manipulation tool and a sphere as the manipulated object. In that work, it was decided to represent only the sphere closest to the cantilever tip. This facilitates the manipulation for untrained users by displaying only important information on the reconstructed scene. The scene is constructed setting 1 Blender unit as 1 μm. All along the operation, the user has complete freedom to modify the camera position and zoom. The drawback of this method is the requirement of prior knowledge of geometries and dimensions and an initial calibration process between real image and virtual reality frames. As in this case the cantilever's and

manipulated objects' geometries are perfectly known and their virtual models are created prior to the operation, it is sufficient to map their real positions to the virtual scene. Details such as the precise shape of the objects, or their exact dimensions are not represented in the virtual scene since this information is not necessary for a manipulation task.

In order to calibrate the real and the virtual cantilever positions, the real cantilever is moved to the contact with substrate, then its vertical position is adjusted such as its flexion is null, without snapping the tip off the surface. This position is offset as the $(0,0,0)$ on the virtual scene. The object position is obtained from image processing along with the tip position. They are then used to calibrate those initial positions with the reference positions of the virtual scene. During the manipulation and after the calibration, the Virtual Reality engine receives periodically positions of the cantilever and the manipulated object and updates them respectively.

Reconstructing a virtual scene using the position information derived with vision algorithm instead of directly transmitting a video of the SEM images enables to decrease the amount of data to transfer, and thus the communication delays.

In addition to 3D display of the scene, haptic feedback is proposed to provide intuitive manipulation environment. Users control the cantilever through a haptic interface, and feel forces which give them information about the scene (Fig. 5). The desired position of the tip $\mathbf{P_t}$ is set using the position of the haptic handle $\mathbf{P_h}$, scaled down by a factor α_p to ensure the precision of the positioning. Operators feel a haptic force $\mathbf{F_h}$ derived from both force measurements and the vision algorithms.

Force measurements, obtained by the flexion of the AFM probe, are used to compute the vertical haptic force f_h^z transmitted to users. It is computed from the vertical force f_t applied on the tip, scaled by a factor α_f to increase it: $f_h^z = \alpha_f f_t$.

To compute the haptic force in the (x, y) plane (substrate plane), vision algorithms are used. They enable to determine the respective position of the tool ($\mathbf{P_t}$) and the sphere ($\mathbf{P_s}$). This force is based only on the distance to the closest sphere. Indeed, simplifying the scene enables the user to concentrate on the manipulation task. Other scenario considering all

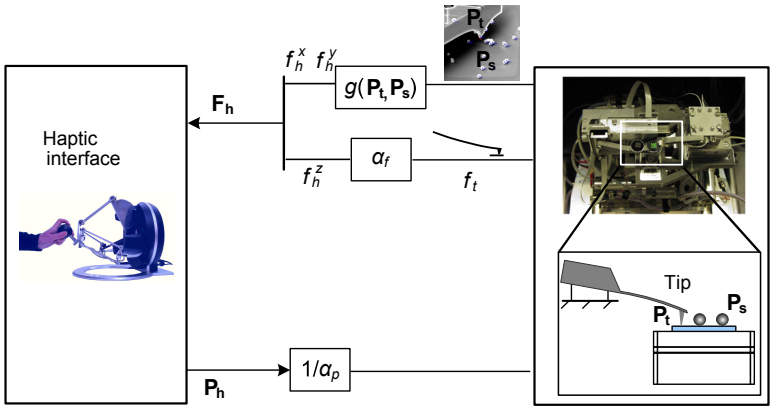

FIGURE 5. Haptic coupling that connects the master device to the AFM manipulator. Users control the tool by using the joystick, and feel in return force feedback. The haptic feedback is computed using both information coming from vision algorithms and direct force measurement of the piezoresistive cantilever.

the objects in a close neighborhood of the tool could be proposed. A repulsive haptic force is computed. It pushes away the tool from the spheres in the horizontal plane and avoid involuntary contact. This force is based on the distance between the tool and the object:

$$\mathbf{D} = \begin{bmatrix} d^x \\ d^y \end{bmatrix} = \begin{bmatrix} p_t^x - p_s^x \\ p_t^y - p_s^y \end{bmatrix} \tag{4.1}$$

where $\|\mathbf{D}\| = \sqrt{d^{x2} + d^{y2}}$ is the distance between the sphere and the tip, and d^x (resp. d^y) are the coordinates along the x (resp. y) axis. Based on that distance, a repulsive force field is computed. While the distance $\|\mathbf{D}\|$ is greater than a given threshold R_{int}, the force is null since it is considered that the tip is far enough from the sphere. When this distance becomes less than the threshold, a non null repulsive force f_r is computed:

$$f_r = \begin{cases} \left(1.0 - \frac{\|\mathbf{D}\|}{R_{int}}\right) f_{max} & \text{if } \|\mathbf{D}\| < R_{int} \\ 0 & \text{else} \end{cases} \tag{4.2}$$

where f_{max} is the maximum force that would be sent for $\|\mathbf{D}\| = 0$. This value will never be reached since the minimum distance between the tip and the center of the sphere cannot be less then the radius of the object. This force enables users to know when they are entering

the interaction radius, and to estimate the relative position of the tip and the sphere for spheres of a given dimension. Moreover, by setting the threshold value equal or slightly superior to the radius of the object, it would also be possible to let the user feel solely the contact in the horizontal plane between the tip and the object.

The force sent to the haptic device is computed by projecting f_r along the x and y axes, proportionally to d^x and d^y. f_h^z is given by measurements of the tip deflection as explained above:

$$\mathbf{F_h} = \begin{bmatrix} f_h^x \\ f_h^y \\ f_h^z \end{bmatrix} = \begin{bmatrix} \frac{d^x}{\|\mathbf{D}\|} f_r \\ \frac{d^y}{\|\mathbf{D}\|} f_r \\ \alpha_f f_t \end{bmatrix} \tag{4.3}$$

4.2. **Intuitive Localization of Microspheres using Remote Teleoperation.** Experiments involving microspheres are conducted through a teleoperated task between France and Germany (Fig. 6). To assist users both visual and haptic indications are provided.

The first indication that users must get is if the tip is or not in contact with the substrate. A repulsive haptic feedback in the vertical direction is then sent to the user in case of contact. Figure 7(a) shows the haptic force sent to the user. Before 10 s the tip is higher than the substrate, and the force felt by the user is null. Then the tip reaches the substrate. The haptic force increases as the user applies a force on the substrate and decreases after 20 s as the user moves the tip upward. The haptic force falls to zero when the tip is moved away from the substrate. The same experiment is performed again after 25 s. The haptic feedback enables users to know when the cantilever is in contact with the substrate, and to estimate the effort applied on the substrate since the haptic force is proportional to the flexion (hence the vertical displacement) of the cantilever.

In addition, users must get information about the relative position of the objects with respect to the tool on the substrate plane. A repulsive haptic feedback as described in Eq . 4.3.

In Fig. 7(b) the user moves the tip around the object, while being in contact with the substrate (a haptic force similar to Fig. 7(a) is also provided but is not depicted here for

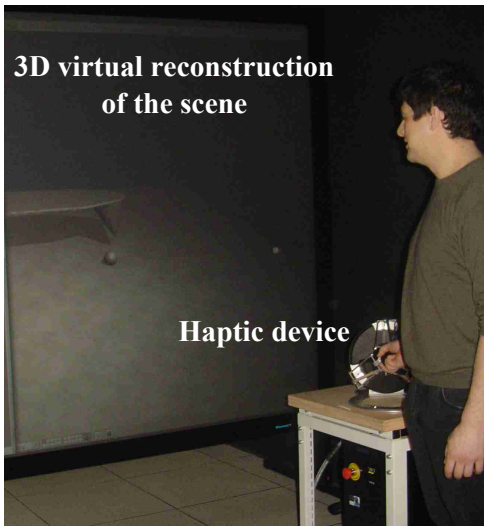

FIGURE 6. Teleoperation of microspheres using a haptic interface, with 3D virtual reconstruction of the manipulation scene. The user manipulates the real AFM, situated in Germany, from the teleoperation facilities in Paris.

the sake of clarity). The position of the sphere as well as the trajectory of the tip are represented. Haptic force on the plane of the substrate is given for several points. The inset represent the simulated haptic force magnitude as a function of the distance between the tip and the closest object. This force tends to keep the tip away from the spheres, and enable users to localize precisely the objects.

The developed vision algorithms enable to provide an intuitive remote manipulation environment composed of both visual and haptic feedback. They are experimentally validated in complex micromanipulation scenes involving hundreds of objects.

5. CONCLUSION

The manipulation of objects smaller than a few micrometers requires the use of Scanning Electron Microscopes. However the visual feedback provided by these systems is not enough to ensure a precise positioning of the tool with respect to the objects, especially when used by non expert operators.

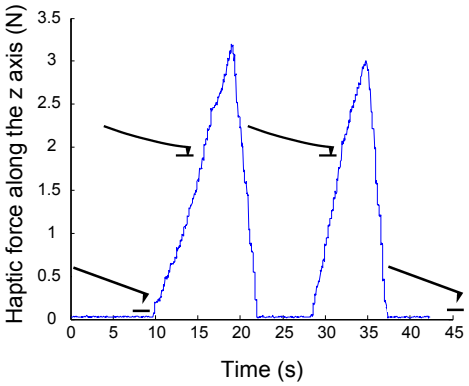

(a) Vertical localization of the cantilever. Scaling factors are set to: $\alpha_p = 4800$, $\alpha_f = 1.10^6$.

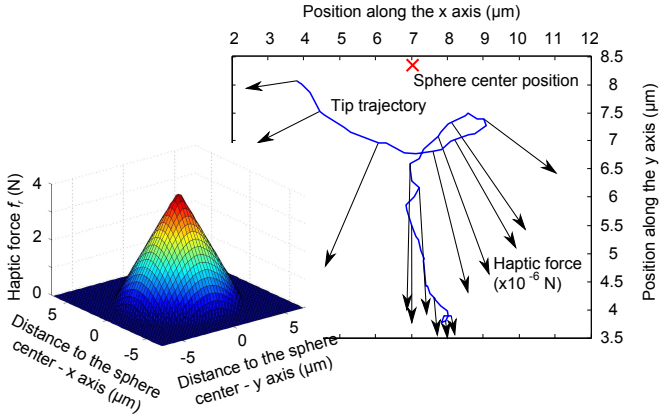

(b) In-plane localization of the spheres. Haptic coupling gains for the force computation are set to: $R_{int} = 5$ µm, $f_{max} = 4$ N, $\alpha_f = 1.10^6$ and $\alpha_p = 4800$. The magnitude of the force vectors is proportional to the distance between the tip and the object (note that x and y scales are different). The inset represents the simulated magnitude of the haptic force f_r.

FIGURE 7. Haptic feedback provided to assist the 3D localization of microspheres.

In this work an intuitive remote teleoperation environment is provided based on information derived from SEM images. The sphere detection algorithm is robust with respect to SEM image issues, such as shadowing, and detects reliably and efficiently micro spheres in complex micromanipulation scenes. To track the tool, a marker based approach is chosen since fast detection is required to provide stable haptic feedback and real time virtual reconstruction of the scene.

The proposed system enables intuitive manipulation of microscale objects from geographically distant sites. The virtual reconstruction of the scene is displayed in stereoscopic view, and haptic feedback is based on both the vision tracking, detection and force measurements. Virtual guides avoid any involuntary collision between the tool and the objects. To widen the range of applications, nanometer size objects should be considered. Other tools, such as grippers, should also be integrated. The reduction of the false positives in vision detection can be done by parameter optimization. Further improvements and optimizations can still decrease the needed computation time. Next step will consist in moving the spheres, for example by pushing them with the cantilever. A special care will be taken to define the manipulation strategy. Several issues, such as sticking effects, must be addressed to perform this manipulation [17].

This work is a first step towards intuitive manipulation environment for microscale objects based on vision algorithms. These systems will offer great opportunities for researchers, giving them access to rare and geographically distant equipments.

6. Acknowledgments

Parts of this work have been funded by the European project FIBLYS and by the project PROCOPE (DAAD-Egide). Special thanks to Uwe Mick for the technical and scientific support.

References

1. F. Beyeler, S. Muntwyler, and B. J. Nelson, *A Six-Axis MEMS Force-Torque sensor with Micro-Newton and Nano-Newtonmeter resolution*, Journal of Microelectromechanical Systems **18** (2009), no. 2, 433–441.
2. Blender, `http://www.blender.org/`.
3. A. Bolopion, C. Stolle, R. Tunnell, S. Haliyo, S. Régnier, and S. Fatikow, *Remote microscale teleoperation through virtual reality and haptic feedback*, IEEE/RSJ International Conference on Intelligent Robots and Systems, 2011, pp. 894–900.
4. A. Bolopion, H. Xie, S. Haliyo, and S. Régnier, *Haptic teleoperation for 3D microassembly of spherical objects*, IEEE/ASME Transaction on Mechatronics **17** (2012), no. 1, 116–127.
5. G. Bradski, *Programmers tool chest: The opencv library*, Dr. Dobbs Journal, November 2000.

6. I. Bukusoglu, C. Basdogan, A. Kiraz, and A. Kurt, *Haptic manipulation of microspheres using optical tweezers under the guidance of artificial force fields*, Presence: Teleoperators and Virtual Environments **17** (2008), no. 4, 344–364.
7. V. Chawda and M. K. O'Malley, *Vision-Based force sensing for nanomanipulation*, IEEE/ASME Transactions on Mechatronics **16** (2011), no. 6, 1177 – 1183.
8. J. Colgate and G. Schenkel, *Passivity of a class of sampled-data systems: Application to haptic interfaces*, Journal of Robotic Systems **14** (1997), no. 1, 37–47.
9. S. Fahlbusch and S. Fatikow, *Force sensing in microrobotic systems-an overview*, International Conference on Electronics, Circuits and Systems, vol. 3, 1998, pp. 259–262 vol.3.
10. A. Ferreira and C. Mavroidis, *Virtual reality and haptics for nanorobotics*, IEEE Robotics and Automation Magazine **13** (2006), no. 3, 78–92.
11. Rafael Gonzales and Richard. Wood, *Digital image processing*, Prentice Hall, Inc., Jersey, USA, 2002.
12. A. Goshtasby, S.H. Gage, and J.F. Bartholic, *A two-stage cross-correlation approach to template matching*, IEEE Trans. Pattern Analysis and Machine Intelligence **6** (1984), no. 3, 374–378.
13. M.A. Greminger and B.J. Nelson, *Vision-based force measurement*, IEEE Transactions on Pattern Analysis and Machine Intelligence **26** (2004), no. 3, 290–298.
14. S. G. Kim and M. Sitti, *Task-based and stable tele-nanomanipulation in a nanoscale virtual environment*, IEEE Trans. on Automation Science and Engineering **3** (2006), no. 3, 240–247.
15. Bradley E. Kratochvil, Lixin X. Dong, and Bradley J. Nelson, *Real-time rigid-body visual tracking in a scanning electron microscope*, International Journal of Robotics Research **28** (2009), no. 4, 498–511.
16. U. Mick, V. Eichhorn, T. Wortmann, C. Diederichs, and S. Fatikow, *Combined nanorobotic afm/sem system as novel toolbox for automated hybrid analysis and manipulation of nanoscale objects*, Proceedings of the IEEE International Conference on Robotics and Automation, 2010, pp. 4088–4093.
17. C.D. Onal and M. Sitti, *Visual servoing-based autonomous 2-D manipulation of microparticles using a nanoprobe*, IEEE Transactions on Control Systems Technology **15** (2007), no. 5, 842–852.
18. C. Pawashe and M. Sitti, *Two-dimensional vision-based autonomous microparticle assembly using nanoprobes*, Journal of Micromechatronics **3** (2006), no. 3-4, 285–306.
19. Annem Narayana Reddy, Nandan Maheshwari, Deepak Kumar Sahu, and G. K. Ananthasuresh, *Miniature compliant grippers with Vision-Based force sensing*, IEEE Transactions on Robotics **26** (2010), no. 5, 867–877.
20. T. Sievers, *Real-time object tracking inside an sem*, Automated Nanohandling by Microrobots (Sergej Fatikow, ed.), Springer Series in Advanced Manufacturing, Springer London, 2008, pp. 103–128.
21. T. Sievers and S. Fatikow, *Real-time object tracking for the robot-based nanohandling in a scanning electron microscope*, Journal of Micromechatronics **3** (2006), no. 3-4, 267–284.

22. Christian Stolle, *Distributed control architecture for automated nanohandling*, International Conference on Informatics in Control, Automation and Robotics (ICINCO'07), 2007, pp. 127–132.

23. N. Trevett, *The open standard for heterogeneous parallel programming*, in Proc. SIGGRAPH (Asia, Singapore), December 2008.

24. T. Wortmann, C. Dahmen, R. Tunnel, and S. Fatikow, *Image processing architecture for real-time micro- and nanohandling applications*, Proc. of the Eleventh IAPR Conference on Machine Vision Applications (MVA) (2009).

25. Hui Xie, C. D Onal, Stéphane Régnier, and Metin Sitti, *Atomic force microscopy based nanorobotics*, modelling, simulation, setup building and experiments series ed., Springer Tracts in Advanced Robotics, vol. 71, 2011.